Insights from in situ and environmental TEM on the oriented attachment of -Fe2O3 nanoparticles during -Fe2O3 nanorod formation

Almeida, Trevor P.; Fay, Michael W.; Hansen, Thomas Willum; Zhu, Yanqiu; Brown, Paul D.

Published in:
CrystEngComm

Link to article, DOI:
10.1039/c3ce41866a

Publication date:
2014

Document Version
Publisher's PDF, also known as Version of record

CrystEngComm

PAPER

Insights from *in situ* and environmental TEM on the oriented attachment of α-Fe_2O_3 nanoparticles during α-Fe_2O_3 nanorod formation

Cite this: *CrystEngComm*, 2014, **16**, 1540

Trevor P. Almeida,†*[a] Michael W. Fay,[b] Thomas W. Hansen,[c] Yanqiu Zhu[d] and Paul D. Brown[a]

Acicular α-Fe_2O_3 nanorods (NRs), at an intermediate stage of development, were isolated using a snapshot valve-assisted hydrothermal synthesis (HS) technique, for the purpose of complementary *in situ* transmission electron microscopy (*i*TEM) and environmental TEM (ETEM) investigations of the effect of local environment on the oriented attachment (OA) of α-Fe_2O_3 nanoparticles (NPs) during α-Fe_2O_3 NR growth. Observations of static snapshot HS samples suggested that α-Fe_2O_3 NPs undergo reorientation following initial attachment, consistent with an intermediate OA stage, prior to 'envelopment' with the developing NR to adopt a perfect single crystal. Conversely, the heating of partially developed α-Fe_2O_3 NRs up to 250 °C, under vacuum, during *i*TEM, demonstrated the progressive coalescence of loosely packed α-Fe_2O_3 NPs and the coarsening of α-Fe_2O_3 NRs, without any direct evidence for an intermediate OA stage. Direct evidence was obtained for the action of an OA mechanism prior to the consumption of α-Fe_2O_3 NPs at the tips of developing α-Fe_2O_3 NRs during ETEM investigation, under an He pressure of 5 mbar at 500 °C. However, α-Fe_2O_3 NPs more strongly attached to the side-walls of developing α-Fe_2O_3 NRs were more likely to be consumed through a local NP destabilisation and reordering process, in the absence of an OA mechanism. Hence, the emerging ETEM evidence suggests a competition between OA and diffusion processes at the α-Fe_2O_3 NP coalescence stage of acicular α-Fe_2O_3 NR crystal development, depending on whether the localised growth conditions facilitate freedom of NP movement.

Received 16th September 2013,
Accepted 1st November 2013

DOI: 10.1039/c3ce41866a

www.rsc.org/crystengcomm

Introduction

One-dimensional (1D) nanostructured materials have attracted considerable research interest due to their many potential applications in the fields of engineering, science and technology.[1] The control of nucleation and propagation in a particular crystallographic direction is central to 1D nanostructure formation,[2] whilst recognising that anisotropic growth is strongly dependent on the nature of the material, and the chemical process and environment of production.

Canted-antiferrimagnetic α-Fe_2O_3 (hematite) is of particular interest as a cheap, environmentally friendly and thermodynamically stable iron oxide, and 1D α-Fe_2O_3 nanorods (NRs) have been investigated for a wide range of applications because their magnetic properties are strongly dependent on NR size and shape.[3] To date, nanostructured α-Fe_2O_3 has been produced using a variety of techniques including sol–gel processing,[4] microemulsion,[5] forced hydrolysis,[6] hydrothermal synthesis (HS)[7] and chemical precipitation.[8] HS, in particular, offers effective control over nanostructure size and shape at relatively low reaction temperatures and short reaction times, providing for well-crystallised reaction products with high homogeneity and definite composition.[9]

Aqueous iron(III) chloride ($FeCl_3$) solution is well established as a simple precursor for the formation of monodispersed α-Fe_2O_3 nanoparticles (NPs),[10] whilst needle-shaped β-FeOOH (akaganeite) NPs are known to form as an intermediate phase during α-Fe_2O_3 NP growth.[11] In particular, a small addition of phosphate (PO_4^{3-}) anions mediates the anisotropic growth of α-Fe_2O_3, leading to the development of acicular NRs through initial size stabilisation (<10 nm) and the oriented attachment (OA) of primary α-Fe_2O_3 NPs.[12] The phosphate mediates the acicular shape of α-Fe_2O_3 NRs during HS at low pH through the absorption of PO_4^{3-} ions on to primary α-Fe_2O_3 NPs in the form of mono or bi-dentate (bridging) surface complexes, on

[a] *Division of Materials, Mechanics and Structures, Department of Mechanical, Materials and Manufacturing Engineering, Faculty of Engineering, University of Nottingham, University Park, Nottingham, NG7 2RD, UK*
[b] *Nottingham Nanotechnology and Nanoscience Centre, University of Nottingham, University Park, Nottingham, NG7 2RD, UK*
[c] *Center for Electron Nanoscopy, Technical University of Denmark, DK-2800 Kgs., Lyngby, Denmark*
[d] *College of Engineering, Mathematics and Physical Sciences, University of Exeter, Streatham Campus, Northcote House, Exeter, EX4 4QJ, UK*
† Present address: Department of Earth Science and Engineering, South Kensington Campus, Imperial College London, London, SW7 2AZ, UK. Tel: +44 (0) 20 759 49983; Email: t.almeida@imperial.ac.uk.

surfaces normal and parallel to the crystallographic α-Fe_2O_3 *c*-axis, respectively.[13,14]

Partial evidence to support this mechanism for acicular α-Fe_2O_3 NR formation has been obtained through the heating of quenched HS intermediate reaction products, *in situ* within a transmission electron microscope (TEM),[15] with the transformation of β-FeOOH NRs into α-Fe_2O_3 NPs during heating in vacuum being consistent with the release of Fe^{3+} ions, through β-FeOOH dissolution, to supply and promote the nucleation and growth of α-Fe_2O_3.

Direct observation of the coarsening of α-Fe_2O_3 NR tips through the consumption and coalescence of primary α-Fe_2O_3 NPs should further support this hydrothermal mechanism for single crystalline acicular α-Fe_2O_3 NR growth. However, it has been found that *in situ* TEM (*i*TEM) heating investigations of the tips of acicular α-Fe_2O_3 NRs, in vacuum, provides limited evidence for the OA of individual α-Fe_2O_3 NPs,[15] highlighting the importance of ambient conditions mediating this part of the growth process. Hence, it is suggested that the addition of a low pressure gas during similar heating investigations in the environmental TEM (ETEM) might favour the dynamic motion of α-Fe_2O_3 NRs, facilitating direct observation of such OA agglomeration mechanisms. In this context, a valve-assisted HS technique is used to provide a snapshot of the acicular α-Fe_2O_3 NRs at a favourable stage of development for OA, and the extent to which *i*TEM and ETEM investigations, under vacuum and low pressure helium ambient, respectively, can be used to examine directly the OA of primary α-Fe_2O_3 NPs, is appraised.

Experimental

Synthesis of α-Fe_2O_3 NRs and NPs

A 'snapshot' view of the growth of primary α-Fe_2O_3 NPs was achieved through the hydrothermal reaction of 0.1 ml 45% pure $FeCl_3$ aqueous solution, further diluted in 20 ml of distilled water (pH ~ 2). The reactant solution was mixed with 1.5 mg of $NH_4H_2PO_4$ surfactant, mechanically stirred in a 50 ml 'valve-assisted' Teflon-lined steel autoclave, and then sealed and inserted into a temperature controlled furnace at 160 °C for 80 min. The autoclave was then removed from the furnace at the reaction temperature and transferred immediately to a tripod support, for stability, where the valve was opened and closed, as quickly as practically possible, for the rapid quenching of sufficient hydrothermal product suspension into liquid nitrogen, as previously described.[16] The resultant suspension comprised frozen droplets, from a few tens of micrometres up to a few millimetres in diameter, with reddish/brown appearance.

Structural characterisation

For the purpose of TEM investigation, tiny frozen droplets expelled from the valve-assisted vessel were deposited straight onto lacey carbon/gold mesh support grids and allowed to melt at room temperature. Conventional diffraction contrast bright field (BF) and high angle annular dark field (HAADF) imaging was performed using an FEI Titan (S)TEM with C_S corrector on the condenser system, operated at 300 kV. Exploratory *i*TEM investigation of α-Fe_2O_3 development as a function of temperature (room temperature to 250 °C at 50 °C intervals), under vacuum, was performed using a Gatan double tilt heating holder within a Jeol 2100F TEM. High resolution phase contrast imaging and ETEM investigation of the oriented attachment mechanism, as a function of temperature (room temperature to 500 °C at 20 °C min^{-1}), under 5 mbar He atmosphere, was performed within an FEI Titan E-Cell TEM with C_S corrector on the objective lens, operated at 300 kV, using a Gatan double tilt heating holder. The elevated temperature of 500 °C, as measured using a thermal couple within the heating holder, was used to help compensate for the low ETEM pressure, being distinct from the high pressure conditions associated with HS *in situ*.

Results

Use of the valve-assisted pressure vessel enables investigation of the near *in situ* HS of aqueous $FeCl_3$ solution. The HAADF and BF TEM images of Fig. 1a–c illustrate the range of α-Fe_2O_3 reaction products formed at 160 °C after 80 min of synthesis, as acquired through rapid quenching. Fig. 1a shows the development of small isotropic primary α-Fe_2O_3 NPs (<10 nm in diameter), whilst Fig. 1b shows a developing α-Fe_2O_3 acicular NR (200 nm long, 40 nm wide). Fig. 1c presents a group of larger, more well-defined, crystalline, acicular α-Fe_2O_3 NRs (~240 nm long, ~40 nm wide) with high aspect ratio.

The high magnification phase contrast TEM images of Fig. 2a–c illustrate the fine detail of the developing filamentary tips of the quenched α-Fe_2O_3 NRs, providing clues as to the localised attachment of individual α-Fe_2O_3 NPs. Fig. 2a illustrates the tip of an α-Fe_2O_3 NR which comprises filamentary features whilst being effectively single crystalline, as confirmed by characteristic lattice fringes (inset). Fig. 2b illustrates the filamentary tip of an α-Fe_2O_3 NR and an attached α-Fe_2O_3 NP which are not in crystallographic alignment, as confirmed by the associated FFT patterns (inset). Conversely, Fig. 2c illustrates the tip of an α-Fe_2O_3 NR and an attached α-Fe_2O_3 NP which are in crystallographic alignment, as evidenced by parallel characteristic {110} lattice fringes (inset).

Similarly, the bright field and phase contrast TEM images of Fig. 3a–c illustrate the alignment of example α-Fe_2O_3 NPs, attached to the sides of the α-Fe_2O_3 NRs. Fig. 3a shows a large acicular α-Fe_2O_3 NR (~400 nm long, ~70 nm wide) with a small α-Fe_2O_3 NP attached to the side (arrowed), magnified in Fig. 3b and identified by its characteristic lattice fringes. In this case, the NP exhibits partial crystallographic alignment with the NR, as evidenced by strong phase contrast fringes for both, but not a perfect, *i.e.* single crystal, crystallographic orientation. Further, Fig. 3c illustrates a couple of small, partially aligned and mis-aligned α-Fe_2O_3 NPs (magnified view inset) attached to a step edge on the side surface of an α-Fe_2O_3 NR.

These combined observations (Fig. 2 and 3) constitute strong evidence for the initial misalignment of attached primary NPs which become progressively crystallographically aligned, to either the tips or sides of the developing α-Fe_2O_3 acicular

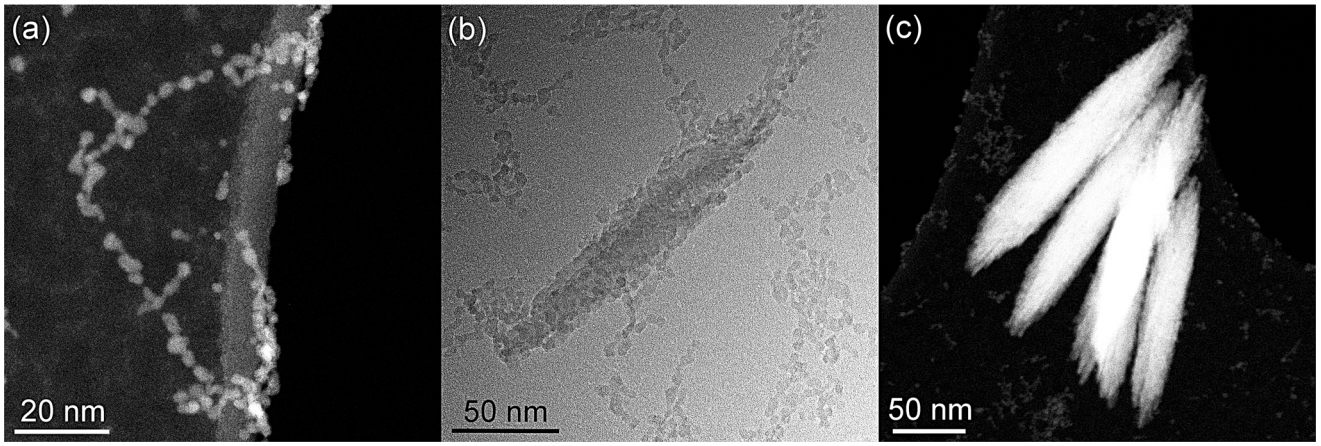

Fig. 1 (a, c) HAADF and (b) BF TEM images of the HS suspension rapidly quenched in liquid nitrogen after heating at 160 °C for 80 minutes. (a) Small primary α-Fe_2O_3 NPs (<10 nm in diameter); (b) developing α-Fe_2O_3 NR (~200 nm long, ~40 nm wide) surrounded by small α-Fe_2O_3 NPs (<10 nm in diameter); and (c) a group of α-Fe_2O_3 NRs (~240 nm long, ~40 nm wide) with filamentary tips.

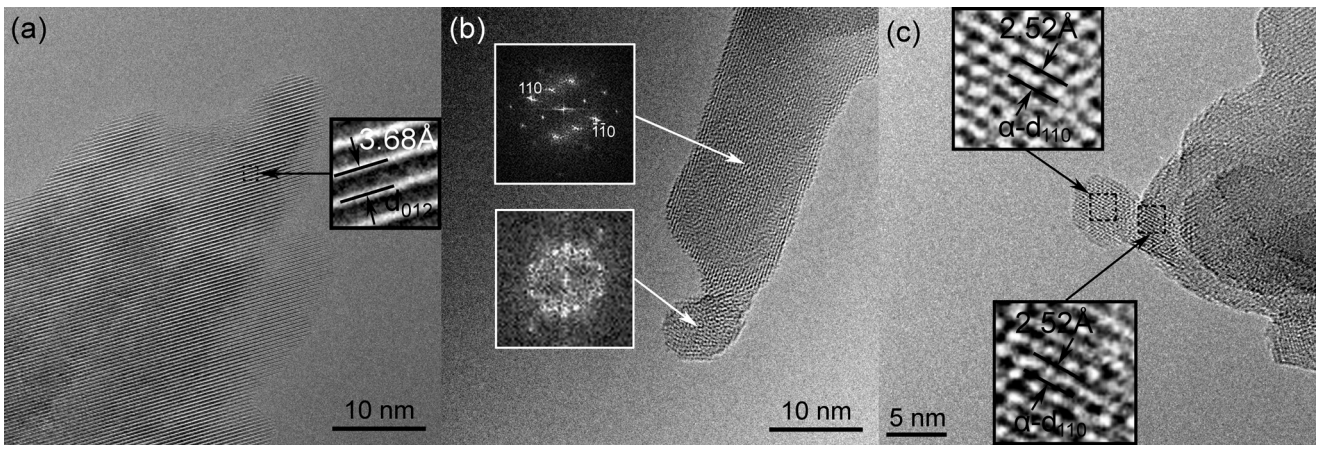

Fig. 2 Phase contrast TEM images of the quenched hydrothermal reaction products synthesised at 160 °C. (a) Filamentary tip of a crystalline α-Fe_2O_3 NR, as identified by characteristic lattice fringes (inset); (b) α-Fe_2O_3 NP attached to the tip of an α-Fe_2O_3 NR, identified and shown to be misaligned by associated FFT (inset); and (c) α-Fe_2O_3 NP attached to the tip of an α-Fe_2O_3 NR, identified and shown to be aligned by characteristic lattice fringes (inset).

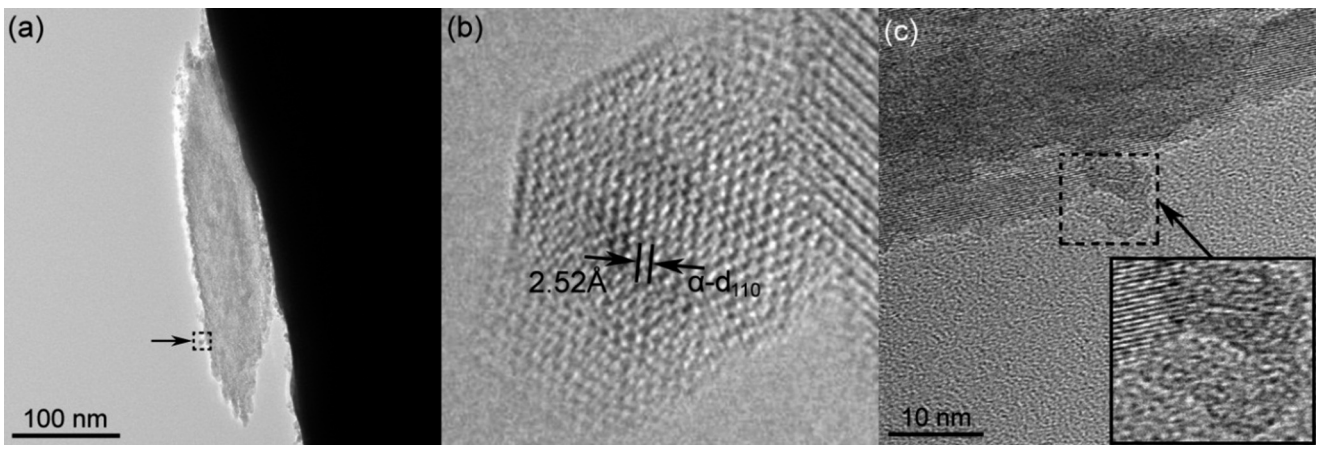

Fig. 3 BF and phase contrast TEM images of the quenched hydrothermal products synthesised at 160 °C. (a) Large acicular α-Fe_2O_3 NR (~400 nm long, ~70 nm wide) with a small α-Fe_2O_3 NP attached to the side (arrowed), and magnified in (b). (c) Small α-Fe_2O_3 NPs (inset) attached to a step edge on the side of a larger α-Fe_2O_3 NR.

NRs, through an OA mechanism.[13] We now consider how *i*TEM and ETEM investigations contribute to this developing understanding.

*i*TEM investigations were conducted initially to seek complementary dynamic information on the growth mechanism of acicular α-Fe_2O_3 NRs.

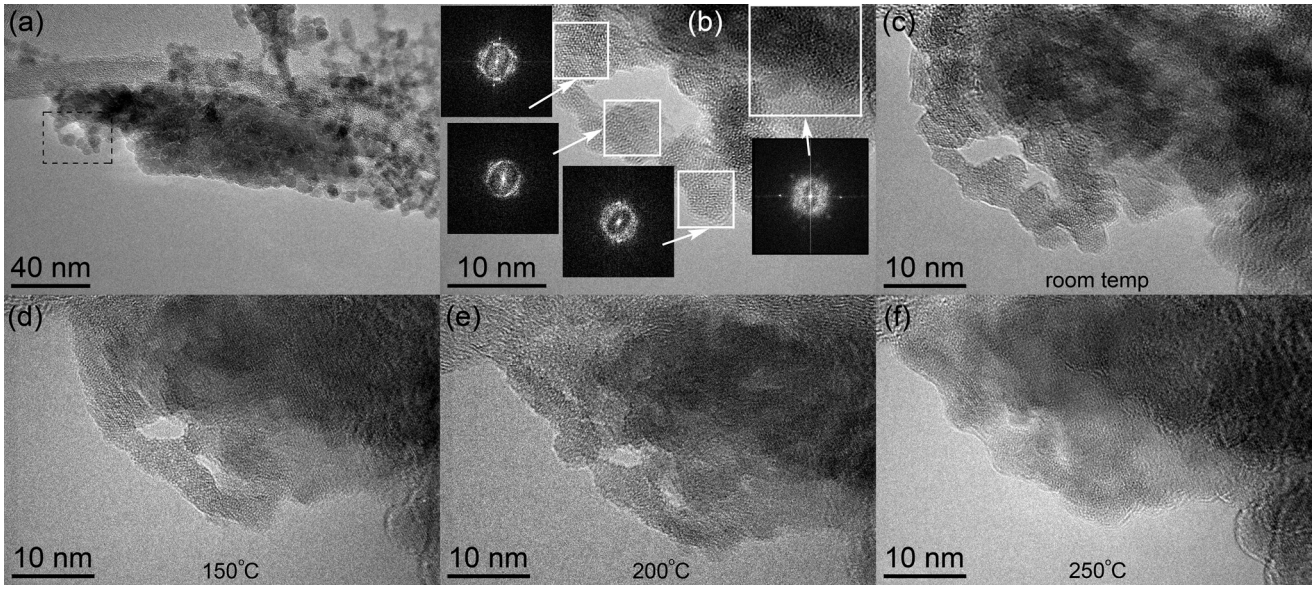

Fig. 4 BF and phase contrast TEM images of the quenched hydrothermal products synthesised at 160 °C. (a) Partially formed acicular α-Fe_2O_3 NR (~200 nm long, ~50 nm wide) with small α-Fe_2O_3 NPs attached to the side of the developing tip (boxed section), and magnified in (b) with FFTs (inset) confirming their random orientations. (c–f) Phase contrast images showing the progressive coalescence and coarsening of these small α-Fe_2O_3 NPs as a function of *in situ* heating: (c) room temperature; (d) 150 °C; (e) 200 °C; and (f) 250 °C.

Fig. 4 presents a series of phase contrast images taken as a function of temperature during the *in situ* TEM heating of α-Fe_2O_3 NPs attached to an α-Fe_2O_3 NR, under vacuum. Fig. 4a shows an acicular α-Fe_2O_3 NR (~200 nm long, ~50 nm wide) with a cluster of small NPs attached to the side of the tip (boxed section). The boxed region of Fig. 4a is magnified in Fig. 4b with inset FFTs showing that the α-Fe_2O_3 NPs exhibited random, dissimilar orientations. Progressive coalescence of the small α-attached Fe_2O_3 NPs and subsequent coarsening of the α-Fe_2O_3 NR was demonstrated following *in situ* heating up to 250 °C (Fig. 4c–f). The heating was performed at a ramp rate of 25 °C min^{-1}, with the electron beam spread, whilst a 5 min dwell period at the 50 °C intervals allowed for sample stabilisation, prior to imaging. However, the coarsening induced by thermal energy, provided *via* the hot stage, did not provide any direct evidence for the OA of individual α-Fe_2O_3 NPs.[15] Hence, investigation of these samples was repeated using a hot stage within an ETEM, again seeking to obtain direct evidence for the dynamic growth of α-Fe_2O_3 acicular NRs through the OA of individual primary α-Fe_2O_3 NPs.

Fig. 5 presents phase contrast images acquired during the process of *in situ* heating within an ETEM under a 5 mbar He atmosphere. Fig. 5a shows a small primary α-Fe_2O_3 NP (arrowed) loosely attached to the tip of a developing α-Fe_2O_3 NR, imaged at room temperature. Fig. 5b, c show selected images from a time-lapse series acquired during an *in situ* heating experiment at 500 °C, demonstrating coarsening and crystallographic growth of the α-Fe_2O_3 NR tip through 'envelopment' of the α-Fe_2O_3 NP.

Similarly, Fig. 6a illustrates a small randomly oriented α-Fe_2O_3 NP attached to the side of a large α-Fe_2O_3 NR, whilst Fig. 6b–d are extracts from a time-lapse series, illustrating the dynamic envelopment of the α-Fe_2O_3 NP, identified by characteristic {110} lattice fringes (inset), during *in situ* heating at 500 °C under 5 mbar He atmosphere. In particular, Fig. 6a illustrates the irregular nature of the side surface of the α-Fe_2O_3 NR, parallel to its major axis, with many step edge positions available for the NP to attach. In this instance, characteristic fringes corresponding to {012} planes within the α-Fe_2O_3 NR are seen to migrate progressively across the smaller α-Fe_2O_3 NP (Fig. 6b–d).

Discussion

The reaction products obtained from the valve-assisted pressure autoclave are considered closely representative of the *in situ* physical state of the developing α-Fe_2O_3 NRs during HS, due to the large cooling rate experienced through quenching. This acts to restrict possible atom/ion transport, thereby locking-in the morphology of the nanostructures.[16] Quenching at a reaction temperature of 160 °C after 80 min of synthesis resulted in the isolation of a reaction product comprising both small primary α-Fe_2O_3 NPs (<10 nm) and larger, partially formed α-Fe_2O_3 acicular NRs (~400 nm long, ~70 nm wide). In the case of conventional HS, it is suggested that Fe^{3+} cations released through intermediate β-FeOOH phase dissolution, prior to primary α-Fe_2O_3 NP formation, may resort back to the reformation of β-FeOOH during the process of conventional cool down, thereby providing a slightly misleading representation of the *in situ* state of the hydrothermal reaction products. Hence, the quenched reaction product shown in Fig. 1 is considered an ideal candidate for static 'snapshot' and dynamic *i*TEM and ETEM investigations of the 'OA stage' of the single crystalline acicular α-Fe_2O_3 NR growth mechanism, and we now consider how these investigations contribute to improved understanding of the attachment and association of primary α-Fe_2O_3 NPs with the developing NRs, in the context of the OA process.

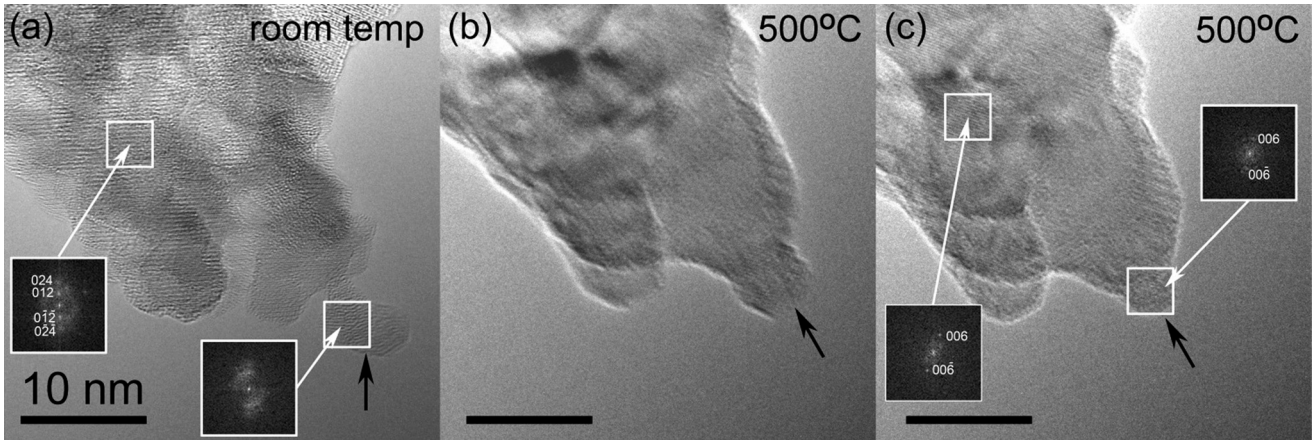

Fig. 5 Phase contrast ETEM images of the hydrothermal reaction products heated to 500 °C under a 5 mbar He atmosphere. (a) Tip of a partially formed α-Fe_2O_3 NR with a small α-Fe_2O_3 NP attached (arrowed), shown to be misaligned by associated FFT (inset). (b, c) Time-lapse phase contrast images (t = 120 s interval between b and c) showing envelopment and alignment of the small α-Fe_2O_3 NP during crystallographic development of the α-Fe_2O_3 NR tip (arrowed), as shown by associated FFT (inset).

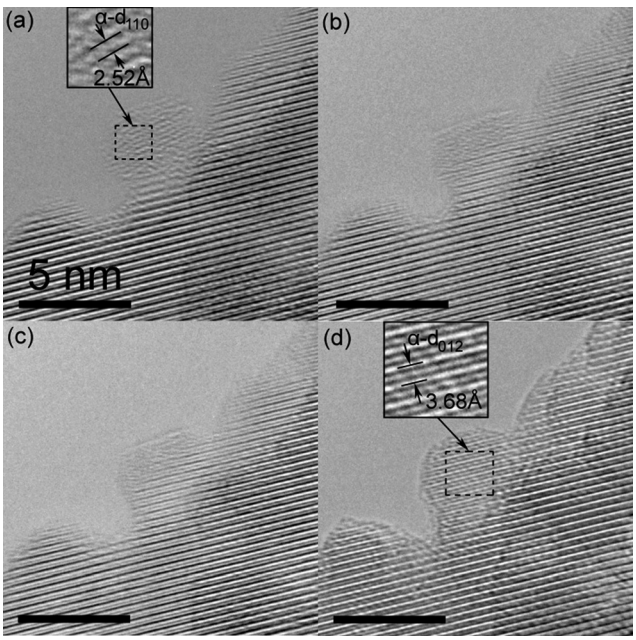

Fig. 6 Phase contrast ETEM images of the hydrothermal reaction products examined at 500 °C under a 5 mbar He atmosphere. (a) Small α-Fe_2O_3 NP attached to the side of a large α-Fe_2O_3 NR, as identified by characteristic lattice fringes (inset). (b–d) Selected time-lapse phase contrast images (t = 30, 60 & 90 s) showing envelopment of the small α-Fe_2O_3 NP onto the side of the large α-Fe_2O_3 NR; {012} lattice fringes are observed to migrate across the smaller α-Fe_2O_3 NP as OA proceeds (d, inset).

The direct observation of α-Fe_2O_3 NPs located either on the tips (Fig. 2) or side surfaces (Fig. 3) of developing α-Fe_2O_3 NRs provides snapshot views of the growth process, at the point of attachment. The example α-Fe_2O_3 NP of Fig. 2c shows it to be crystallographically aligned with the tip of a developing α-Fe_2O_3 NR. In contrast, the α-Fe_2O_3 NPs shown in Fig. 2b, 3b and c, attached either to NR tip or side-walls, were found to be partially crystallographically aligned or randomly oriented, suggesting that the NPs might be more generally misaligned at the initial point of attachment to the NRs, before adopting a stronger crystallographic association. Hence, the investigation of snapshot HS samples suggests that the NPs undergo reorientation following initial attachment, consistent with an OA mechanism, prior to a process of 'envelopment' with the developing NR to adopt a perfect single crystal.

Direct observation of the coarsening of the tips of α-Fe_2O_3 NRs through the consumption and coalescence of clustered α-Fe_2O_3 NPs (Fig. 4) was provided by time-lapse imaging during the *in situ* heating of quenched samples within the *i*TEM. The caveat being that these localised transformations occurred under vacuum rather than within aqueous media during HS in the presence of phosphate surfactant. Nevertheless, the observation of coalescence of loosely packed α-Fe_2O_3 NPs (Fig. 4c) and the coarsening of the α-Fe_2O_3 NR (Fig. 4f) at elevated temperature is still supportive of the model proposed for the formation of acicular α-Fe_2O_3 NRs, albeit without direct evidence for the action of an intermediate OA mechanism.

However, additional observations of the envelopment of primary α-Fe_2O_3 NPs on the tip and side surfaces of an α-Fe_2O_3 NR, as provided by time-lapse imaging during ETEM investigation under an He atmosphere at 500 °C (Fig. 5 & 6), provides a slightly different perspective of this stage of growth. Fig. 5 constitutes direct evidence for the operation of an OA mechanism for the case of a primary α-Fe_2O_3 NP attaching to a NR tip, promoted by *in situ* heating at elevated temperature under He gas ambient conditions, prior to the processes of envelopment. However, the evidence from Fig. 6 indicates an alternative process of localised diffusion and recrystallisation of a randomly oriented primary α-Fe_2O_3 NP attached to the side of a developing α-Fe_2O_3 NR, to adopt perfect single crystal alignment, without an intermediate OA process involving mechanistic realignment and crystallographic reorientation of the attaching NP. Hence, the emerging ETEM evidence suggests there might be a competition between OA and diffusion processes at the coalescence stage of NP attachment and NR crystal development, depending on the localised growth conditions.

With regard to the technical details of the OA mechanism, under conventional HS conditions,[13] a grain-rotation-induced grain coalescence (GRIGC) mechanism[17,18] is considered to minimize the area of high energy interfaces, allowing low-energy configurations to become established, eliminating misoriented grain boundaries and forming coherent grain-grain boundaries, in accordance with the model proposed by Zhang *et al.*[19] In the case of HS, at low pH, it is considered that the GRIGC mechanism is mediated by absorbed phosphate surfactant anions, whereby PO_4^{3-} absorbs strongly to planes parallel to the α-Fe_2O_3 *c*-axis in a bi-dentate (bridging) fashion, in preference to weaker mono-dentate PO_4^{3-} absorption, which would be more easily disrupted during NR growth.[13]

This crystallographic dependence for absorption retards the ability of new material, *e.g.* in the form of primary α-Fe_2O_3 NPs, to attach to developing α-Fe_2O_3 nanostructure faces parallel to the *c*-axis, ultimately resulting in the development of filamentary features which crystallographically align to define the shape of the acicular α-Fe_2O_3 NRs.[13] This type of mechanistic OA aggregation is known to produce slightly porous α-Fe_2O_3 NR HS reaction products which retain traces of both water and phosphate surfactant.[9,20] The extent to which *i*TEM and ETEM investigations contribute to this developing understanding of the OA mechanism during HS growth is now considered.

There are clear distinctions between the mechanisms of α-Fe_2O_3 NR development elucidated from the observation of snapshot HS samples, and the evidence provided from the localised *i*TEM and ETEM investigation of developing NRs at elevated temperature. Time lapse *i*TEM imaging with increasing temperature (Fig. 4) showed progressive coalescence of a group of randomly attached primary α-Fe_2O_3 NPs to produce a coarsened, compacted α-Fe_2O_3 NR tip. However, whilst thermal annealing in this instance promoted α-Fe_2O_3 NP coalescence, there was no direct evidence for an active stage of NP reorientation to allow favourable coherent grain–grain configurations to be formed. Conversely, the evidence provided by the ETEM investigations at elevated temperature provided direct evidence for the OA of an individual α-Fe_2O_3 NP located at the tip of an α-Fe_2O_3 NR (Fig. 5). During heating, the initially randomly aligned α-Fe_2O_3 NP (Fig. 5a) was observed to reorient and adhere more strongly in crystallographic alignment with the developing α-Fe_2O_3 NR (Fig. 5b), and subsequently decrease in size (Fig. 5c), indicative of diffusion and recrystallization processes during this latter stage of envelopment to form a perfect single crystal.

Conversely, the randomly oriented α-Fe_2O_3 NP positioned on the side surface of the α-Fe_2O_3 NR shown in Fig. 6 was found to maintain its original size whilst becoming crystallographically aligned with the α-Fe_2O_3 NR, in this case just through a process of diffusion and recrystallization, without any direct evidence for an OA mechanism (Fig. 6d). Hence, the tip and side α-Fe_2O_3 NPs are consumed in slightly different ways by the developing α-Fe_2O_3 NR, depending on whether local conditions allow OA to proceed freely prior to envelopment. Thus, in the case of tip attachment, the direct evidence from ETEM indicates that the α-Fe_2O_3 NP reorients and adheres crystallographically to the NR, through an OA process, prior to becoming consumed through a local ripening process at the NR tip. Conversely, it is considered that side attached α-Fe_2O_3 NPs are more strongly attached at step-edges, limiting the prospects for localised OA prior to consumption, again by a localised ripening process whereby the surface of the NP at the attachment interface becomes unstable, with progressive reordering of the NP, on a layer by layer basis, to achieve crystallographic alignment with the NR.

Thus, the *i*TEM and ETEM investigations have provided evidence for the localised agglomeration, coarsening and consumption of primary α-Fe_2O_3 NPs, in support of the general model for the growth of acicular α-Fe_2O_3 NRs. However, the consumption of α-Fe_2O_3 NPs is not necessarily proceeded by a process of OA, which is strongly dependent on whether the localised conditions facilitate freedom of NP movement. However, the strong indication is that of a localised process of NP crystal lattice destabilisation and reordering through a process of elemental migration leading and ripening, or a process of progressive crystallographic realignment and localised diffusion, leading to the development of single crystal α-Fe_2O_3 NRs. It is now recognised that combined *i*TEM and ETEM investigations, in conjunction with the investigation of snapshot HS samples at intermediate stages of α-Fe_2O_3 NR growth, are needed to unravel the fine details of such growth mechanisms. In this context, it is recognised that more work is needed to elucidate the role of *e.g.* pH and PO_4^{3-} absorption on the shape development of α-Fe_2O_3 nanostructures, in order to identify their optimum conditions growth.

Conclusions

Partially developed 'snapshot' α-Fe_2O_3 NRs, isolated using a valve-assisted HS reaction vessel, have been used to facilitate investigation of the OA stage of α-Fe_2O_3 NPs attachment to α-Fe_2O_3 NRs, as a function of the local environment, using the complementary techniques of *i*TEM and ETEM. The combined investigations have provided direct evidence for the localised agglomeration, coarsening and consumption of primary α-Fe_2O_3 NPs, in support of the general model for acicular α-Fe_2O_3 NR growth. In particular, direct observation of the OA stage of α-Fe_2O_3 NP attachment was obtained using ETEM, for the case of α-Fe_2O_3 NPs consumed at the tips of developing α-Fe_2O_3 NRs. NPs more strongly attached to the side-walls of the NRs were found to be consumed by a local diffusion and recrystallization process, in the absence of an OA mechanism. Hence, it is suggested that there is a competition between local OA and diffusion processes at the coalescence stage of α-Fe_2O_3 NP attachment and α-Fe_2O_3 NR crystal development, depending on whether the localised growth conditions facilitate freedom of NP movement.

Acknowledgements

The authors would like to thank the EPSRC for financial support.

Notes and references

1 S. Kuchibhatla, A. S. Karakoti, D. Bera and S. Seal, *Prog. Mater. Sci.*, 2007, **52**, 699–913.
2 Y. Xia, P. Yang, Y. Sun, Y. Wu, B. Mayers, B. Gates, Y. Yin, F. Kim and H. Yan, *Adv. Mater.*, 2003, **15**, 353–389.
3 Z. Jing and S. Wu, *Mater. Lett.*, 2004, **58**, 3637–3640.
4 X. Q. Liu, S. W. Tao and Y. S. Shen, *Sens. Actuators, B*, 1997, **40**, 161–165.
5 D. O. Yener and H. Giesche, *J. Am. Ceram. Soc.*, 2001, **84**(9), 1987–1995.
6 Q. Li and Y. Wei, *Mater. Res. Bull.*, 1998, **33**, 779–782.
7 X. Liu, G. Qiu, A. Yan, Z. Wang and X. Li, *J. Alloys Compd.*, 2007, **433**, 216–220.
8 R. D. Zysler, M. Vasquez-Mansilla, C. Arciprete, M. Dimitrijewits, D. Rodriguez-Sierra and C. Saragovi, *J. Magn. Magn. Mater.*, 2001, **224**, 39–48.
9 T. P. Almeida, M. Fay, Y. Zhu and P. D. Brown, *J. Phys. Chem. C*, 2009, **113**, 18689–18698.
10 T. Sugimoto, K. Sakata and A. Muramatsu, *J. Colloid Interface Sci.*, 1993, **159**, 372–382.
11 T. Sugimoto and A. Muramatsu, *J. Colloid Interface Sci.*, 1996, **184**, 626–638.
12 T. Sugimoto, A. Muramatsu, K. Sakata and D. Shindo, *J. Colloid Interface Sci.*, 1992, **158**, 420–428.
13 T. P. Almeida, M. Fay, Y. Zhu and P. D. Brown, *Nanoscale*, 2010, **2**, 2390–2398.
14 E. J. Elzinga and D. L. Sparks, *J. Colloid Interface Sci.*, 2007, **308**, 53–70.
15 T. P. Almeida, M. Fay, Y. Zhu and P. D. Brown, *Physica E*, 2012, **44**, 1058–1061.
16 T. P. Almeida, M. Fay, Y. Zhu and P. D. Brown, *CrystEngComm*, 2010, **12**, 1700–1704.
17 D. Moldovan, V. Yamakov, D. Wolf and S. R. Phillpot, *Phys. Rev. Lett.*, 2002, **89**, 20.
18 E. R. Leite, T. R. Giraldi, F. M. Pontes and E. Longo, *Appl. Phys. Lett.*, 2003, **83**, 1566–1568.
19 J. Zhang, F. Huang and Z. Lin, *Nanoscale*, 2009, **2**, 18–34.
20 L. Suber, D. Fiorani, P. Imperatori, S. Foglia, A. Montone and R. Zysler, *Nanostruct. Mater.*, 1999, **11**, 797–803.